Accepted for publication in The Astronomical Journal

The Nature of Boxy/Peanut-Shaped Bulges in Spiral Galaxies

M. Bureau[1] and K. C. Freeman
Research School of Astronomy and Astrophysics, Institute of Advanced Studies, The Australian National University, Mount Stromlo and Siding Spring Observatories, Private Bag, Weston Creek P.O., ACT 2611, Australia

ABSTRACT

We present a systematic observational study of the relationship between bars and boxy/peanut-shaped (B/PS) bulges. We first review and discuss proposed mechanisms for their formation, focussing on accretion and bar-buckling scenarios. Using new methods relying on the kinematics of edge-on disks, we then look for bars in a large sample of edge-on spiral galaxies with a B/PS bulge and in a smaller control sample of edge-on spirals with more spheroidal bulges. We present position-velocity diagrams of the ionised gas obtained from optical long-slit spectroscopy. We show that almost all B/PS bulges are due to a thick bar viewed edge-on, while only a few extreme cases may be due to the accretion of external material. This strongly supports the bar-buckling mechanism for the formation of B/PS bulges. None of the galaxies in the control sample shows evidence for a bar, which suggests conversely that bars are generally B/PS.

We consider the effects of dust in the disk of the galaxies, but conclude that it does not significantly affect our results. Unusual emission line ratios correlating with kinematical structures are observed in many objects, and we argue that this is consistent with the presence of strong bars in the disk of the galaxies. As expected from N-body simulations, the boxy–peanut transition appears to be related to the viewing angle, but more work is required to derive the precise orientation of the bars the bulges.

The reliable identification of bars in edge-on spiral galaxies opens up for the first time the possibility of studying observationally the vertical structure of bars.

Subject headings: galaxies: formation — galaxies: evolution — galaxies: kinematics and dynamics — galaxies: structure — galaxies: spiral — instabilities

---

[1]Now at Sterrewacht Leiden, Postbus 9513, 2300 RA Leiden, The Netherlands

1. Introduction

Many spiral galaxies display boxy or peanut-shaped bulges when viewed edge-on. Unfortunately, statistical studies of the incidence of these objects have not used objective criteria to quantify the boxiness of the bulges, and they are therefore hard to compare and yield moderately different results. Nevertheless, it seems clear that at least 20-30% of edge-on spirals possess a boxy/peanut-shaped (hereafter B/PS) bulge (see Jarvis 1986; Shaw 1987; de Souza & dos Anjos 1987). Spiral galaxies with a B/PS bulge are therefore a significant class of objects.

The fact that the boxy/peanut shape is seen only in edge-on spirals indicates that the shape is related to the vertical distribution of light. Compared to the usual $R^{1/4}$ light distribution of spheroids, B/PS bulges have excess light above the plane at large galactocentric radii (see Shaw 1993). Furthermore, the three-dimensional (hereafter 3D) light distribution of B/PS bulges must be even more extreme than their projected surface brightness (see, e.g., Binney & Petrou 1985 for axisymmetric models). B/PS bulges also appear to rotate cylindrically, i.e. their rotation is independent of the height above the plane (e.g. Kormendy & Illingworth 1982; Rowley 1986).

Several models have been proposed to explain the structure of B/PS bulges (e.g. Combes & Sanders 1981; May, van Albada, & Norman 1985; Binney & Petrou 1985). However, despite their prevalence and interesting structural and dynamical properties, B/PS bulges remain poorly studied observationally, probably because the edge-on projection makes the interpretation of observational data difficult.

In this paper, we present new kinematical data for a large sample of spiral galaxies with a B/PS bulge. Our main goals are to determine their 3D structure and to identify their likely formation mechanism. We use our data to show that B/PS bulges are simply thick bars viewed edge-on.

In § 2, we discuss the two main scenarios proposed for the formation of B/PS bulges – accretion of satellite galaxies and buckling of a bar. We describe ways of discriminating between the two scenarios using kinematical data in § 3. The observations are presented in § 4 and the results discussed at length in § 5. We conclude in § 6.

2. Formation Mechanisms

2.1. Accretion

Accretion of external material such as satellite galaxies was the early favoured mechanism to explain the formation of B/PS bulges in spiral galaxies. Binney & Petrou (1985) and Rowley (1986, 1988) showed that it is possible to construct axisymmetric cylindrically rotating B/PS bulges from relatively simple distribution functions. Binney & Petrou adopted a distribution function with a third integral of motion, in addition to the energy E and angular momentum along the symmetry axis L_z. This integral favoured orbits reaching a particular height above the plane. Rowley adopted a two-integral distribution function, with a truncation depending on both E and L_z. Both authors argued that the required distribution functions can form naturally through the accretion of material onto a host spiral galaxy. Binney & Petrou (1985) additionally argued that, for the accreted material to form a B/PS bulge, the velocity dispersion of the satellite must be much lower than its orbital speed, and the decay timescale must be much longer that the orbital time. This ensures that the accreted material stays clustered in phase space.

Accretion scenarios face several problems. At one extreme, one can consider the accretion of several small satellite galaxies. However, only a narrow range of orbital energy and angular momentum can lead to the formation of a B/PS bulge, so it is improbable that many satellite galaxies would all share these properties. Remaining satellites should then be present but they are not observed (Shaw 1987). The accretion of a single large companion is also ruled out by the large velocity dispersion and small decay timescale involved (Binney & Petrou 1985). Similarly, the merger of two spiral galaxies of similar sizes (or of a spiral and a small elliptical) seems an unlikely route to form B/PS bulges. This would require a fairly precise alignment of the spins and orbital angular momenta of the two galaxies. We recall that about a third of all spiral galaxy bulges should be formed this way.

From the arguments presented above, it seems that the accretion of a small number of moderate-sized satellites is the only accretion scenario which may lead to the formation of B/PS bulges. In favour of accretion is the fact that the best examples of B/PS bulges are found in small groups (e.g. NGC 128, ESO 597- G 036). In addition, the possibly related X-shaped galaxies can form through the accretion of a satellite galaxy (e.g. Whitmore & Bell 1988; Hernquist & Quinn 1989). On the other hand, no evidence of accretion (arcs, shells, filaments, etc.) were detected by Shaw (1993) near spirals with a B/PS bulge, which argues against any kind of accretion. Furthermore, spiral galaxies with a B/PS bulge are not found preferentially in clusters (Shaw 1987). We are thus led to the conclusion that, while accretion of external material may play a role in the formation of some B/PS bulges, it is unlikely to be the primary formation mechanism.

2.2. Bar-Buckling

Bars can form naturally in N-body simulations of rotationally supported stellar disks (e.g. Sellwood 1981; Athanassoula & Sellwood 1986), due to global bisymmetric instabilities (e.g. Kalnajs 1971, 1977). Based on 3D N-body simulations, Combes & Sanders (1981) were the first to suggest that B/PS bulges may arise from the thickening of bars in the disks of spiral galaxies. Their results were confirmed and their suggestion supported by later works (see, e.g., Combes et al. 1990; Raha et al. 1991). In short, the simulations show that, soon after a bar develops, it buckles and settles with an increased thickness and vertical velocity dispersion, appearing boxy-shaped when seen end-on and peanut-shaped when seen side-on. The B/PS bulges so formed are cylindrically rotating, as required.

Toomre (1966) first considered the buckling of disks, in highly idealised models, and found that, if the vertical velocity dispersion in a disk is less than about a third of the velocity dispersion in the plane, the disk will be unstable to buckling modes (fire-hose or buckling instability; see also Fridman & Polyachenko 1984; Araki 1985). Bar formation in a disk makes the orbits within the bar more eccentric without affecting much their perpendicular motions, thereby providing a natural mechanism for the bar to buckle. Resonances between the rotation of the bar and the vertical oscillations of the stars can also make the disk vertically unstable (see Pfenniger 1984; Combes et al. 1990; Pfenniger & Friedli 1991). Irrespective of exactly how a bar buckled, the final shape of the bar is probably due to orbits trapped around the 2:2:1 periodic orbit family (see, e.g., Pfenniger & Friedli 1991).

Bar-buckling is the currently favoured mechanism for the formation of B/PS bulges. In particular, it provides a natural way to form B/PS bulges in isolated spiral galaxies, which accretion scenarios are unable to do. A number of facts also suggest a connection between (thick) bars and B/PS bulges, although they do not support bar-*buckling* directly. In particular, the fraction of edge-on spirals possessing a B/PS bulge is similar to the fraction of strongly barred spirals among face-on systems ($\approx 30\%$; see, e.g., Sellwood & Wilkinson 1993; Shaw 1987). In a few cases, a bar can also be directly associated with a B/PS bulge from morphological arguments. NGC 4442 is such an example (Bettoni & Galletta 1994).

The main observational problem faced by the bar-buckling mechanism is that B/PS bulges seem to be shorter (relative to the disk diameter) than real bars or the strong bars formed in N-body simulations. However, this might simply be due to projection (a given surface brightness level being reached at a smaller radius in a more face-on disk) and no proper statistics have yet been compiled. The long term secular evolution of bars is also poorly understood. For example, it is known that bars can transfer angular momentum to a spheroidal component very efficiently (e.g. Sellwood 1980; Weinberg 1985). On the other hand, Debattista & Sellwood (1998) showed that, while a bar can be slowed down, it continues to grow and the boxy/peanut shape is preserved. It is less clear what happens if a bar is strongly perturbed. However, Norman, Sellwood, & Hasan (1996) showed that, if a bar is destroyed through the growth of a central mass concentration (e.g. Hasan & Norman 1990; Friedli & Benz 1993), the boxy/peanut shape is also destroyed.

The merits of the bar-buckling mechanism significantly outweigh these potential problems, and the bar-buckling scenario to form B/PS bulges remains largely unchallenged at the moment, despite very little observational support. The main aim of this paper is to test this mechanism, by looking for bars in a large sample of spiral galaxies with a B/PS bulge. Although this stops short of a direct verification of buckling, it does test directly for a possible relationship between bars and B/PS bulges. We will come back to this distinction in § 5.

Although it is not part of our program, the Milky Way is a primary example of such a galaxy. The Galactic bulge is boxy-shaped (Weiland et al. 1994) and it is now well established that it is bar-like (e.g. Binney et al. 1991; Paczyński et al. 1994; see Kuijken 1996 for a brief review of the subject).

We note that "hybrid" scenarios have also been proposed to explain the formation of B/PS bulges, and have gathered recent support from statistical work on the environment of B/PS bulges by Lütticke & Dettmar (1998). An interaction or merger can excite (or accelerate) the development of a bar in a disk which is stable (or quasi-stable) against bar formation (e.g. Noguchi 1987; Gerin, Combes, & Athanassoula 1990; Miwa & Noguchi 1998). Bars formed this way are then free to evolve to a boxy/peanut shape in the manner described above (see, e.g., Mihos et al. 1995), and the bulges thus formed owe as much to interactions as they do to the bar-buckling instability. However, the *shape* of the bulges is due to the buckling of the bars and interaction is merely a way to start the bar formation process. In that sense, hybrid scenarios for the formation of B/PS bulges are really bar-buckling scenarios, and the possible accretion of material is not directly related to the issue of the bulges' shape.

3. Observational Diagnostics

Our main goal with the observations presented in this paper is to look for the presence of a bar in the disk of spiral galaxies possessing a B/PS bulge. There is no straightforward photometric way to identify a bar in an edge-on spiral. The presence of a plateau in the major-axis light profile of the disk has often been invoked as an indicator of a bar (e.g. de Carvalho & da Costa 1987; Hamabe & Wakamatsu 1989). However, axisymmetric or quasi-axisymmetric features (e.g. a lens) can be mistaken for a bar and end-on bars may remain undetected. Kuijken & Merrifield (1995; see also Merrifield 1996) were the first to demonstrate that bars could be identified kinematically in external edge-on spiral galaxies. They showed that periodic orbits in a barred galaxy model produce characteristic double-peaked line-of-sight velocity distributions when viewed edge-on. This gives their modeled spectra a spectacular "figure-of-eight" (or X-shaped) appearance, which they were able to observe in the long-slit spectra of the B/PS systems NGC 5746 and NGC 5965 (see Fig. 1 for examples). Their approach is analogous to that used in the Galaxy with longitude-velocity diagrams (e.g. Peters 1975; Mulder & Liem 1986; Binney et al. 1991).

Bureau & Athanassoula (1999, hereafter BA99) refined the dynamical theory of Kuijken & Merrifield (1995). They used periodic orbit families in a barred galaxy model as building blocks to model the structure and kinematics of real galaxies. They showed that the global structure of a position-velocity diagram[2] (hereafter PVD) taken along the major axis of an edge-on system is a reliable bar diagnostic, particularly the presence of gaps between the signatures of the different families of periodic orbits. Athanassoula & Bureau (1999, hereafter AB99) produced similar bar diagnostics using hydrodynamical simulations of the gaseous component alone. They showed that, when x_2 orbits are present (corresponding to the existence of an inner Lindblad resonance (hereafter ILR)), the presence of gaps in a PVD, between the signature of the x_2-like flow and that of the outer parts of the disk, reliably indicates the presence of a bar. If no x_2 orbits are present, one must rely on indirect evidence to argue for the presence of a bar (see, e.g., Contopoulos & Grosbøl 1989 for a review of periodic orbits in barred spirals). The gaps are a direct consequence of the shocks which develop in relatively strong bars. These shocks drive an inflow of gas toward the center of the galaxies and deplete the outer (or entire) bar regions (see, e.g., Athanassoula 1992). The simulations of AB99 can be directly compared with the emission line spectra presented here, and will form the basis of our argument.

The models of BA99 and AB99 can also be used to determine the viewing angle with

---

[2]Position-velocity diagrams (PVDs) show the projected density of material in a system as a function of line-of-sight velocity and projected position.

respect to a bar, as the signature present in the PVDs changes with the orientation of the line-of-sight. In particular, when a bar is seen end-on, the x_1 orbits (and x_1-like flow, both elongated parallel to the bar) reach very high radial velocities, while the x_2 orbits (and x_2-like flow, both elongated perpendicular to the bar) show only relatively low velocities. The opposite is true when a bar is seen side-on. In addition, the presence or absence of x_2 orbits can somewhat constrain the mass distribution and bar pattern speed of an observed galaxy.

We have not developed specific observational criteria to identify past or current accretion of material in the observed galaxies. As discussed in § 2.1, accretion will occur through interactions or merger events. We will take as the signature of such events, and of possible accretion, the presence of irregularities in the observed PVDs, in particular strong asymmetries about the center of an object (see Fig. 1 for examples).

4. Observations

4.1. The Sample

Our sample of galaxies consists of 30 edge-on spirals selected from the catalogues of Jarvis (1986), Shaw (1987), and de Souza & dos Anjos (1987) (spiral galaxies with a B/PS bulge), and from the catalogue of Karachentsev, Karachentseva, & Parnovsky (1993) (spirals with extreme axial ratios; see also Karachentsev et al. 1993). In order to have enough spatial resolution in the long-slit spectroscopy, but still be able to image the galaxies relatively quickly with a small-field near-infrared (hereafter NIR) camera, we have selected objects with bulges larger than $0\farcm6$ in diameter and disks smaller than about $7\farcm0$ (at the 25 B mag arcsec^{-2} level). NIR imaging is important to refine the classification of the bulges and to subsequently study the vertical structure of the identified bars. All objects are accessible from the south ($\delta \leq 15°$). Three-quarters (23/30) of the galaxies either have probable companions or are part of a group or cluster. A few of these probably are chance alignments, so it is fair to say that we are not biased either against or for galaxies in a dense environment. We should therefore be able to estimate reliably the importance of accretion in the formation of B/PS bulges.

Of the sample galaxies described above, 80% (24/30) have a boxy or peanut-shaped bulge, while 20% (6/30) have a more spheroidal bulge morphology and constitute a "control" sample. Of the former group, it turned out that 17 galaxies have emission lines extending far enough in the disk to apply the diagnostics developed by BA99 and AB99 with the ionised gas; all galaxies in the control group fulfill this condition. In this paper, we will thus concentrate on a main sample of 17 edge-on spiral galaxies with a B/PS bulge and a comparison sample of 6 edge-on spiral galaxies with more spheroidal bulges. The galaxies in each sample are listed in Tables 1 and 2 respectively, along with information on their properties and environment. The galaxies with no or confined emission are listed in Table 3. For those, stellar kinematics must be used to search for the presence of bar. We note that the galaxy type listed in Tables 1–3 is not precise to more than one or two morphological type, because of the difficulty of classifying edge-on spirals. The bulge-to-disk ratio is effectively the only criterion left to classify the objects.

Other than the catalogue of Karachentsev et al. (1993), we are not aware of any general catalogue of edge-on spiral galaxies. This makes it difficult to build a large and varied control sample including edge-on spiral galaxies with large bulges (the Karachentsev et al. 1993 catalogue is restricted to galaxies with major to minor axis ratio $a/b \geq 7$). Such a catalogue would be very useful, and could probably be constructed from an initial list of candidates taken from a catalogue such as the RC3 (de Vaucouleurs et al. 1991), which would then be inspected on survey material.

4.2. Observations and Data Reduction

Our spectroscopic data were acquired between December 1995 and May 1997 (total of 39 nights) using the Double Beam Spectrograph on the 2.3 m telescope at Siding Spring Observatory. A 1752×532 pixels SITE ST-D06A thinned CCD was used. The observations discussed in this paper were obtained with the red arm of the spectrograph centered on the Hα λ6563 emission line. All galaxies were observed using a $1\farcs8 \times 400''$ slit aligned with the major axis. For objects with a strong dust lane, the slit was positioned just above it. The spectral resolution is about 1.1 Å FWHM (0.55 Å pixel^{-1}) and the spatial scale is $0\farcs9$ pixel^{-1}. These data can be directly compared with the gas dynamical models of AB99.

When no emission line was detected in an object, the red arm of the spectrograph was moved to the Ca II absorption line triplet. The blue arm was always centered on the Mg b absorption feature. These data will form the core of a future paper discussing stellar kinematics in the sample galaxies (including the galaxies in Table 3). Total exposure times on both arms ranged from 12000 to 21000 s on each object.

The spectra were reduced using the standard procedure within IRAF. The data were first bias-subtracted, using both vertical and horizontal overscan regions, and then using bias frames. If necessary, the data were also dark-subtracted. The spectra were then flatfielded using flattened continuum lamp exposures, and wavelength-calibrated using bracketing arc lamp exposures for each image. The data were then rebinned to a logarithmic wavelength (linear velocity) scale corresponding to 25 km s^{-1} $pixel^{-1}$. The spectra were then corrected for vignetting along the slit using sky exposures. All exposures of a given object were then registered and offset along the spatial axis, corrected to a heliocentric rest frame, and combined. The resulting spectra were then sky-subtracted using source-free regions of the slit on each side of the objects. The sky subtraction was less than perfect in some cases, mainly because of difficulties in obtaining a uniform focus of the spectrograph along the entire length of the slit. This was particularly troublesome for objects like IC 2531 and NGC 5746 which have sizes comparable to that of the slit (see, e.g., Fig. 3a). In order to isolate the emission lines, the continuum emission of the objects was then subtracted using a low-order fit to the data in the spectral direction. The resulting spectra constitute the basis of our discussion in the next section.

We note that in regions with bright continuum emission, like the center of some galaxies, the continuum subtraction can leave high shot noise in the data, which should not be confused with line emission in the grayscale plots of Figure 1–3. This is the case for example in the spectra of ESO 240- G 011, NGC 1032, and NGC 4703. The effect is perhaps best seen when a bright star is subtracted, such as in the spectra of NGC 2788A or NGC 1032 (see Fig. 1).

We have not extracted rotation curves from our data. This is because the entire two-dimensional spectrum, or PVD, is required to identify the signature of a bar in an edge-on spiral galaxy (see BA99 and AB99). Evidence of interaction and of possible accretion of material is also more easily seen in the PVDs. We present the [N II] λ6584 emission line rather than Hα because it is not affected by underlying stellar absorption.

4.3. Results

We present the emission line spectrum for the sample galaxies which have extended emission only. The PVDs of the galaxies in the main sample and the control sample are shown in Figure 1 and Figure 2, respectively. In order to illustrate the range of galaxy type and bulge morphology in the sample, and to allow connections to be made between bulge morphologies and kinematical features in the disks, each PVD is accompanied by a registered image of the corresponding galaxy (from the Digitized Sky Survey) on the same spatial scale. We discuss here the trends observed across the data set.

The most important trend, and the main result of this paper, is that most galaxies in the main sample show a clear bar signature in their PVD (as described in § 3). Of the 17 galaxies in the main sample of spirals with a B/PS bulge and extended emission lines, we conclude that 14 are barred. In these objects, the PVD clearly shows a strong and steep inner component, associated with an x_2-like flow, and a slowly-rising almost solid-body component, associated with the outer disk, and joining the flat section of the rotation curve in the outer parts. The two components are separated by a gap, caused by the absence (or low density) of gaseous material with x_1-like kinematics in the outer bar regions[3]. The best examples of this type of bar signature are seen in the PVD of earlier-type objects, like NGC 2788A, NGC 5746, and IC 5096. However, the signature is still clearly visible in the PVD of galaxies as late as ESO 240- G 011.

In the main sample, only one galaxy, NGC 4469, may be axisymmetric, with no evidence of either a bar or interaction (although it is not possible to rule out an interaction which would have occured a long time ago, leaving no observable trace). Two galaxies, NGC 3390 and ESO 597- G 036, have a disturbed strongly asymmetric PVD, which we ascribe to a recent interaction (obvious in the case of ESO 597- G 036). These interactions may have led to the accretion of material. The results for the entire main sample are summarised in Table 1.

Another significant result of this study is that no galaxy in the control sample shows evidence for a bar. Four of the six galaxies appear to be axisymmetric, without evidence for either a bar or interaction, and two galaxies (NGC 5084 and NGC 7123) have a disturbed PVD, indicating they underwent an interaction recently and possibly accreted material. These results are tabulated in Table 2.

5. Discussion

5.1. The Structure of Boxy/Peanut-Shaped Bulges

The only previous study of this kind was that of Kuijken & Merrifield (1995), who proposed the method and considered two galaxies; Bureau & Freeman (1997) presented preliminary results of the current work. This is thus the first systematic observational study of the relationship between bars and B/PS bulges. In summary, our main result is that, based on new kinematical data, 14 of the 17 galaxies with a B/PS bulge in our sample are barred, and the remaining 3 galaxies show evidence of interaction or may be axisymmetric. None of the 6 galaxies without a B/PS bulge in our sample shows any indication of a bar.

---

[3]The PVDs of NGC 128 and IC 2531 do not display a bar signature, but Emsellem & Arsenault (1997) and Bureau & Freeman (1997) showed, using other data, that each galaxy harbours a bar.

This means that most B/PS bulges are due to the presence of a thick bar viewed edge-on, and only a few may be due to the accretion of external material. In addition, the more spheroidal bulges (i.e. non-B/PS) do seem axisymmetric. It appears then that most B/PS bulges are edge-on bars, and that most bars are B/PS when viewed edge-on. However, the small size of the control sample prevents us from making a stronger statement about this converse. There is also a continuum of bar strengths in nature and we would expect to have intermediate cases. The galaxies NGC 3957 and NGC 4703 may represent such objects: one could argue that their PVDs display weak bar signatures, and indeed their bulges are the most flattened in the control sample.

If bars were unrelated to the structure of bulges, we would have expected only about 5 galaxies in the main sample to be strongly barred, and about 2 galaxies in the control sample (about 30% of spirals are strongly barred, Sellwood & Wilkinson 1993). Clearly, our results are incompatible with these expectations. Recent results by Merrifield & Kuijken (1999) also support our conclusions. Based on a smaller sample of northern edge-on spirals, they show clearly that as bulges become more B/PS, the complexity and strength of the bar signature in the PVD also increase.

Our association of bars and B/PS bulges supports the bar-buckling mechanism for the formation of the latter. However, we do not test directly for buckling, but rather for the presence of a barred potential in the plane of the disks. Because bars form rapidly and buckle soon after, on a timescale of only a few dynamical times (see, e.g., Combes et al. 1990), it is unlikely that any galaxy in this nearby sample would have been caught in the act. Thus, other mechanisms which could lead to thick bars cannot be excluded. In addition, we have no way of determining how the bars themselves formed, or even whether they formed spontaneously in isolation or through interaction with nearby galaxies or companions. Therefore, the possibility of hybrid scenarios for the formation of B/PS bulges, where a bar is formed because of an interaction and subsequently thickens due to the buckling instability, remains (see § 2.2).

We have looked mainly at objects with large bulges; only two of the galaxies studied are late-type spirals (ESO 240- G 011 and IC 5176). This is a selection effect due to the difficulty to identify very small B/PS bulges. It would therefore be interesting to search for bars in very late edge-on spiral galaxies, and verify whether thin bars do exist: the bar in ESO 240- G 011 is not very thick, but it is thicker (isophotally) than the disk. H I synthesis imaging is probably the best way to achieve this goal, as these objects are often dusty and H I-rich. Such bars may even provide a novel way to constrain the total (luminous and dark) mass distribution of spirals, in a manner analogous to the use of warps or flaring, as buckling is sensitive to the presence of a dark halo (e.g. Combes & Sanders 1981). We will report on H I synthesis observations of a few objects in our sample in a later paper.

Our observations revive the old issue of the exact nature of bulges. In face-on systems, one can often clearly identify a bar and a more nearly axisymmetric component usually referred to as the bulge. However, Kormendy (1993) has argued that, at least in some examples, these apparent bulges may just be structures in the disk. In edge-on spirals, we are not aware of any galaxies displaying two separate vertically extended components. This raises the question of whether the bars and bulges of face-on systems are really two distinct structural and dynamical components, despite the fact that they can be separated photometrically. Our data on edge-on galaxies tightly link the presence of a bar with the presence of a B/PS bulge, which suggests that bars and B/PS bulges are very closely related. This view is supported by theoretical and modelling work on barred spiral galaxies (e.g. Pfenniger 1984; Pfenniger & Friedli 1991), as well as by some photometric studies (e.g. Ohta 1996). However, more work is required to settle the issue. Kinematical data covering whole bulges would be particularly useful.

BA99 and AB99 proposed diagnostics, again based on the structure of the observed PVD, to determine the viewing angle with respect to a bar in an edge-on disk (see § 3). When the bar is seen close to side-on, the maximum line-of-sight velocity reached by the x_2-like flow is similar to or larger than the flat portion of the rotation curve, and the component of the PVD associated with that flow is very steep. When the bar is seen close to end-on, the x_2-like flow only reaches low velocities and extends to relatively large projected distances. These diagnostics are ideally suited to test the main prediction of N-body models, that bars are peanut-shaped when seen side-on and boxy-shaped when seen end-on (see, e.g., Combes & Sanders 1981; Raha et al. 1991).

Of the 12 barred galaxies in the main sample for which it is possible to apply these criteria (we exclude NGC 128 and IC 2531), two-thirds (8/12) seem to be consistent with the above prediction of N-body simulations. For example, in the galaxy with a peanut-shaped bulge IC 4937, it is clear that the steep inner component associated with the x_2-like flow extends to higher velocities than the outer parts of the disk (see Fig. 1). This situation is reversed in NGC 1886, which has a boxy-shaped bulge. However, caution is required when interpreting this result. Firstly, the present classification of the shape of the bulges is affected by both dust and the low dynamic range of the material used (Digitized Sky Survey). To remedy this problem, we have acquired K-band images of all the sample galaxies and will report on these observations in a future paper. Secondly, no clear prediction has been made from N-body simulations about the viewing angle at which the transition from a boxy to a peanut-shaped bulge occurs. In that regard, it would be useful to apply quantitative measurements of the boxiness and "peanutness" of the bulges to both simulation results and observational data (see, e.g., Bender & Möllenhoff 1987 and Athanassoula et al. 1990 for two possible methods). Thirdly, because the x_2-like flow is located near the center of the galaxies, the velocities it reaches depend somewhat on the central concentration of the objects (which affects the circular velocity in the central regions). This obviously varies significantly amongst the galaxies in our sample. Therefore, while our observations may support the prediction of N-body models concerning the orientation of the bar in B/PS bulges, we believe that it is premature to make a detailed quantitative comparison of the data with the models.

For a more detailed comparison with theory, data of higher signal-to-noise and higher spatial resolution than the average PVD presented here would be very desirable. However, it would be worthwhile to model individually the best PVDs obtained in the present study (e.g. NGC 5746, IC 5096, and a few others). This would very likely lead to tight constraints on the mass distribution and bar properties of the galaxies, including the orientation and pattern speed of the bars (see BA99; AB99). The K-band images could also be used to constrain the mass distributions. Comparing the data with the kinematics (or simply the rotation curve) predicted from an axisymmetric deprojection would provide an easy test of the shape of the bulges. On a related subject, the significant thickness of bars suggests that their 3D structure should be taken into account when deriving the potential of more face-on systems from NIR images.

In that regard, we should stress that the bar diagnostics we used rely on the presence of an x_2-like flow in the center of the galaxies, and thus on the existence of ILRs (or, at least, one ILR; see BA99; AB99). A priori, barred disks or B/PS bulges need not have ILRs, but at least 13 of the 17 galaxies in the main sample do (we additionally exclude NGC 128 here). Our data therefore strongly support the view that barred spiral galaxies generally have ILRs (see also Athanassoula 1991, 1992).

5.2. Dust and Emission Line Ratios in Boxy/Peanut-Shaped Bulges

Because many galaxies in our sample have a prominent dust lane, it is important to consider the effects dust may have on our observations. Its principal consequence in edge-on systems is to limit the depth to which the line-of-sight penetrates the disk. To bypass this problem, we selected many galaxies to be slightly inclined, so it was possible in those objects to position the slit just above the dust lane and have a line-of-sight that still goes through most of the disk, as required for a comparison with the models of BA99 and AB99. In the few cases with a strong dust lane and a perfectly edge-on disk, we tried again to offset the slit slightly. Unfortunately, with the observational set-up available at the telescope, it was difficult to position the slit with great precision. The objects where we suspected that dust could affect our observations are indicated in Tables 1–3. A large dust optical depth produces an almost featureless PVD, as one sees only an outer annulus of material in the disk, and the rotation curve appears slowly-rising and solid-body (see, e.g., Bosma et al. 1992). The only objects showing obvious signs of extinction are IC 2531[4], NGC 4703, and possibly ESO 443- G 042. Because we see a lot of structure in most PVDs, including the PVDs of objects with a significant dust lane, we do not believe that our results are significantly affected by dust. We do detect a clear bar signature in most galaxies in the main sample.

This statement is strengthened by the fact that all the PVDs showing a bar signature are close to symmetric. AB99 showed that the bar signature would be strongly asymmetric in a very dusty disk, and this is not observed. Similarly, it is improbable that irregular dust distributions would lead to such well-ordered and symmetric PVDs (very large and localized dust "patches" would be required to create the important gaps observed in many objects).

An unexpected but interesting prospect raised by our observations concerns emission line ratios. For many of the barred galaxies in the main sample, the emission line ratios in the central regions are different from those expected of typical H II regions. For 9 barred galaxies out of 14, mostly those with the strongest bar signatures, the [N II] λ6584 to Hα λ6563 ratio in the bulge region is greater than unity. In particular, in a few objects, the steep inner component of the PVD, associated with the x_2-like flow, is much stronger in [N II] than it is in Hα, while the slowly rising component, associated with the outer disk, has a [N II]/Hα ratio typical of H II regions. In fact, the inner component can be almost absent in Hα. We illustrate these behaviours in Figure 3, which shows the PVDs of the galaxies NGC 5746 and IC 5096 in the Hα and [N II] $\lambda 6548, 6584$ lines.

It is possible that the Hα emission line is weakened by the underlying stellar absorption. This suggestion is supported by the fact that the spectra of many of the galaxies in the main sample show strong Balmer absorption lines. However, the Hα absorption would need to be very large to account for the extreme [N II]/Hα ratios observed in some objects (e.g. IC 5096). The strong Balmer lines observed in many objects are nevertheless interesting in themselves, and indicate that a significant intermediate age ($\sim$ 1 Gyr) stellar population is present in the central regions of the disk of many of the galaxies. It would be interesting to investigate if these past bursts of star formation can be related to the presence of the bars.

The high emission line ratios are interesting for two reasons. Firstly, high [N II]/Hα

[4]This is confirmed by the H I radio synthesis data of Bureau & Freeman (1997), which reveal a complex PVD with a bar signature.

ratios are commonly believed to be produced by shocks (see, e.g., Binette, Dopita, & Tuohy 1985; Dopita & Sutherland 1996). This is consistent with the view that B/PS bulges are barred spirals viewed edge-on. The steep inner components of the PVDs, which display high [N II]/Hα ratios, are associated with an x_2-like flow and the nuclear spirals observed in many barred spiral galaxies (AB99). Athanassoula (1992) showed convincingly that these are the locus of shocks. Secondly, if one were to derive Hα and [N II] rotation curves from the data, by taking the upper envelope of the PVDs (the standard method), the Hα and [N II] rotation curves would significantly differ for many objects. The [N II] lines would yield rapidly rising rotation curves flattening out at small radii, while the Hα line would yield slowly rising rotation curves flattening out at relatively large radii. Mass models derived from such data would thus yield qualitatively different results, and our understanding of galactic dynamics and structure gained from this type of work could be seriously erroneous (at least for highly inclined spirals). Of course, now that these galaxies are known to be barred, their rotation curves should not be used directly for mass modelling, as they are not a good representation of the circular velocity.

Data such as those presented in Figure 3 also open up the possibility of determining the ionisation conditions and abundance of the gas in different regions of the galaxies in a single observation. Because the deprojected location of each component of the PVDs is known (see AB99), this provides an efficient way to study the effects of bars on the interstellar medium of galaxies on various scales.

6. Conclusions

In this paper, we discussed the various mechanisms proposed for the formation of the boxy and peanut-shaped bulges observed in some edge-on spiral galaxies. We argued that accretion scenarios were unlikely to account for most boxy/peanut-shaped (B/PS) bulges, but that bar-buckling scenarios, discovered through N-body simulations, had this potential. Using recently developed kinematical bar diagnostics, we searched for bars in a large sample of edge-on spiral galaxies with a B/PS bulge. Of the 17 galaxies where the diagnostics could be applied using emission lines, 14 galaxies were shown to be barred, 2 galaxies were significantly disturbed, and 1 galaxy seemed to be axisymmetric. In a control sample of 6 galaxies with spheroidal bulges, none appeared to be barred.

Our study supports the bar-buckling mechanism for the formation of B/PS bulges. Our results imply that most B/PS bulges are due to the presence of a thick bar that we are viewing edge-on, while only a few may be due to the accretion of external material. Furthermore, spheroidal bulges do appear to be axisymmetric. This suggests that all bars are B/PS. Our observations also seem to support the main prediction of N-body simulations, that bars appear boxy-shaped when seen end-on and peanut-shaped when seen side-on. However, this issue should be revisited in a more quantitative manner in the future. With our data, we have no way of determining whether the bars leading to B/PS bulges have formed in isolation or through interactions and mergers. The association of B/PS bulges and bars is entirely consistent with the properties of the bulge of the Milky Way, which is known to be both boxy and bar-like.

We considered the effects of dust on our observations, but concluded that it does not affect our results significantly. We have also shown that emission line ratios correlate with kinematical structures in many barred galaxies. This make possible a direct study of the large scale effects of bars on the interstellar medium in disks.

Our study opens up the possibility to study observationally the vertical structure of bars. This was not possible before and represents an interesting spin-off from the use of bar diagnostics in edge-on spiral galaxies. To this end, we have obtained K-band images of all our sample galaxies, and will report on this work in a future paper.

We thank the staff of Mount Stromlo and Siding Spring Observatories for their assistance during and after the observations. We also thank A. Kalnajs, E. Athanassoula, A. Bosma, and L. Sparke for useful discussions. M. B. acknowledges the support of an Australian DEET Overseas Postgraduate Research Scholarship and a Canadian NSERC Postgraduate Scholarship during the conduct of this research. The Digitized Sky Surveys were produced at the Space Telescope Science Institute under U.S. Government grant NAG W-2166. The images of these surveys are based on photographic data obtained using the Oschin Schmidt Telescope on Palomar Mountain and the UK Schmidt Telescope. The plates were processed into the present compressed digital form with the permission of these institutions. The NASA/IPAC Extragalactic Database (NED) is operated by the Jet Propulsion Laboratory, California Institute of Technology, under contract with the National Aeronautics and Space Administration.

REFERENCES

Araki, S. 1985, Ph.D. Thesis, Massachusetts Institute of Technology

Athanassoula, E. 1991, in Dynamics of Disk Galaxies, ed. B. Sundelius (CTH: Göteborg), 149

———. 1992, MNRAS, 259, 345

Athanassoula, E., & Bureau, M. 1999, ApJ, submitted.

Athanassoula, E., Morin, S., Wozniak, H., Puy, D., Pierce, M. J., Lombard, J., & Bosma, A. 1990, MNRAS, 245, 130

Athanassoula, E., & Sellwood, J. A. 1986, MNRAS, 221, 213

Bender, R., & Möllenhoff, C. 1987, A&A, 177, 71

Bettoni, D., & Galletta, G. 1994, A&A, 281, 1

Binette, L., Dopita, M. A., & Tuohy, I. R. 1985, ApJ, 297, 476

Binney, J. J., Gerhard, O. E., Stark, A. A., Bally, J., & Uchida, K. I. 1991, MNRAS, 252, 210

Binney, J., & Petrou, M. 1985, MNRAS, 214 449

Bosma, A., Byun, Y., Freeman, K. C., & Athanassoula, E. 1992, ApJ, 400, L21

Bureau, M., & Athanassoula, E. 1999, ApJ, in press.

Bureau, M., & Freeman, K. C. 1997, PASA, 14, 146

Combes, F., Debbasch, F., Friedli, D., & Pfenniger, D. 1990, A&A, 233, 82

Combes, F., & Sanders, R. H. 1981, A&A, 96, 164

Contopoulos, G., & Grosbøl, P., 1989, A&A Rev., 1, 261

Debattista, V. P., & Sellwood, J. A. 1998, ApJ, 493, L5

de Carvalho, R. R., & da Costa, L. N. 1987, A&A, 171, 66

de Souza, R. E., & dos Anjos, S. 1987, A&AS, 70, 465

de Vaucouleurs, G., de Vaucouleurs, A., Corwin, H. G. Jr., Buta, R. J., Paturel, G., Fouque, P. 1991, Third Reference Catalogue of Bright Galaxies (Springer-Verlag: New York)

Dopita, M. A., & Sutherland, R. S. 1996, ApJS, 102, 161

Emsellem, E., & Arsenault, R. 1997, A&A, 318, L39

Fridman, A. M., & Polyachenko, V. L. 1984, Physics of Gravitating Systems (Springer-Verlag: New York)

Friedli, D., & Benz, W. 1993, A&A, 268, 65

Gerin, M., Combes, F., & Athanassoula, E. 1990, A&A, 230, 37

Hamabe, M., & Wakamatsu, K. 1989, ApJ, 339, 783

Hasan, H., & Norman, C. 1990, ApJ, 361, 69

Hernquist, L., & Quinn, P. J. 1989, ApJ, 342, 1

Jarvis, B. J. 1986, AJ, 91, 65

Kalnajs, A. J. 1971, ApJ, 166, 275

———. 1977, ApJ, 212, 637

Karachentsev, I. D., Karachentseva, V. E., & Parnovsky, S. L. 1993, Astron. Nachr., 314, 97

Karachentsev, I. D., Karachentseva, V. E., Parnovsky, S. L., & Kudrya, Y. N. 1993, Astron. & Astrophys. Trans., 4, 143 Kormendy, J. 1993, in Galactic Bulges, ed. H. DeJonghe, and H. J. Habing (Kluwer: Dordrecht), 209

Kormendy, J., & Illingworth, G. 1982, ApJ, 256, 460

Kuijken, K. 1996, in Barred Galaxies, ed. R. Buta, D. A. Crocker, and B. G. Elmegreen (ASP: San Francisco), 505

Kuijken, K., & Merrifield, M. R. 1995, ApJ, 443, L13

Lütticke, R., & Dettmar, R.-J. 1998, in When and How do Bulges Form and Evolve?, ed. C. M. Carollo, H. C. Ferguson, and R. F. G. Wyse (Cambridge University Press: Cambridge), in press.

May, A., van Albada, T. S., & Norman, C. A. 1985, MNRAS, 214 131

Merrifield, M. R. 1996, in Barred Galaxies, ed. R. Buta, D. A. Crocker, and B. G. Elmegreen (ASP: San Francisco), 179

Merrifield, M. R., & Kuijken, K. 1999, MNRAS, submitted.

Mihos, J. C., Walker, I. R., Hernquist, L., de Oliveira, M. C., & Bolte, M. 1995, ApJ, 447, L87

Miwa, T., & Noguchi, M. 1998, ApJ, 499, 149

Mulder, W. A., & Liem, B. T. 1986, A&A, 157, 148

Noguchi, M. 1987, MNRAS, 228, 635

Norman, C. A., Sellwood, J. A., & Hasan, H. 1996, ApJ, 462, 114

Ohta, K. 1996, in Barred Galaxies, ed. R. Buta, D. A. Crocker, and B. G. Elmegreen (ASP: San Francisco), 37

Paczyński, B., Stanek, K. Z., Udalski, A., Szymański, M., Kałużny, J., Kubiak, M., Mateo, M., & Krzemiński, W. 1994, ApJ, 435, L113

Peters, W. L. 1975, ApJ, 195, 617

Pfenniger, D. 1984, A&A, 134, 373

Pfenniger, D., & Friedli, D. 1991, A&A, 252, 75

Raha, N., Sellwood, J. A., James, R. A., & Kahn, F. D. 1991, Nature, 352, 411

Rowley, G. 1986, Ph.D. Thesis, The Australian National University

———. 1988, ApJ, 331, 124

Sellwood, J. A. 1980, A&A, 89, 296

———. 1981, A&A, 99, 362

Sellwood, J. A., & Wilkinson, A. 1993, Rep. Prog. Phys., 56, 173

Shaw, M. A. 1987, MNRAS, 229, 691

———. 1993, MNRAS, 261, 718

Toomre, A. 1966, in Geophysical Fluid Dynamics, 1966 Summer Study Program at Woods Hole Oceanographic Institution, ref. no. 66-46, 111

Weiland, J. L., et al. 1994, ApJ, 425, L81

Weinberg, M. D. 1985, MNRAS, 213, 451

Whitmore, B. C., & Bell, M. 1988, ApJ, 324, 741

This preprint was prepared with the AAS LaTeX macros v4.0.

Fig. 1.— Structure and kinematics of the galaxies in the main sample of spirals with a boxy/peanut-shaped bulge. Each plot corresponds to a galaxy. For each, the top panel shows a blue image of the galaxy (identified in the bottom-left corner) from the Digitized Sky Survey, and the bottom panel shows an ionised gas ([N II] λ6584 emission line) position-velocity diagram (PVD) taken along the major axis, and registered with the image above it. The galaxies are ordered as in Table 1.

Fig. 2.— Same as Figure 1 but for the control sample of galaxies (Table 2).

Fig. 3.— Structure and kinematics of (a) NGC 5746 and (b) IC 5096. For each galaxy, the top panel shows a blue image of the galaxy from the Digitized Sky Survey, and the bottom panel shows ionised gas position-velocity diagrams (PVDs) taken along the major axis, and registered with the image above them. The PVDs correspond to the [N II] λ6584, Hα λ6563, and [N II] λ6548 emission lines (from top to bottom). Note the large [N II] λ6584 to Hα ratio in the inner steep component of the PVDs.

Table 1. Main Sample (Detections)

Galaxy	Type	Bulge	Environment	Structure	Notes
NGC 128	S0 pec	Peanut	In group	Bar[a]	...
ESO 151- G 004	$S0^0$	Peanut	In group	Bar	...
NGC 1886	Sab	Boxy	Isolated	Bar	...
NGC 2788A	Sb	Peanut	In cluster	Bar	Dusty
IC 2531	Sb	Peanut	In cluster	Bar[b]	Dusty
NGC 3390	Sb	Boxy	Companions?	Accretion	...
NGC 4469	SB(s)0/a?	Peanut	In cluster	Axisymmetric	...
NGC 4710	$SA(r)0^+$	Boxy	In cluster	Bar	...
PGC 44931	Sbc	Peanut	Isolated	Bar	...
ESO 443- G 042	Sb	Peanut	Companions?	Bar	Dusty
NGC 5746	SAB(rs)b?	Peanut	In group	Bar	...
NGC 6722	Sb	Peanut	Isolated	Bar	...
NGC 6771	$SB(r)0^+$?	Peanut	In group	Bar	...
IC 4937	Sb	Peanut	In cluster	Bar	Dusty
ESO 597- G 036	$S0^0$ pec	Peanut	In group	Accretion	Dusty
IC 5096	Sb	Boxy	Companions?	Bar	...
ESO 240- G 011	Sb	Boxy	In group	Bar	...

[a]Emsellem & Arsenault (1997)

[b]Bureau & Freeman (1997)

Table 2. Control Sample

Galaxy	Type	Bulge	Environment	Structure	Notes
NGC 1032	S0/a	Spheroidal	Companions?	Axisymmetric	Dusty
NGC 3957	$SA0^{+}$	Spheroidal	In cluster	Axisymmetric	⋯
NGC 4703	Sb	Spheroidal	Isolated	Axisymmetric	Dusty
NGC 5084	S0	Spheroidal	In cluster	Accretion	⋯
NGC 7123	Sa	Spheroidal	Isolated	Accretion	Dusty
IC 5176	SAB(s)bc?	Spheroidal	Companions?	Axisymmetric	⋯

Table 3. Main Sample (Non-Detections)

Galaxy	Type	Bulge	Environment	Notes
NGC 1381	SA0	Boxy	In cluster	⋯
NGC 1596	SA0	Boxy	In group	⋯
NGC 2310	S0	Boxy	Isolated	⋯
ESO 311- G 012	S0/a?	Boxy	Isolated	⋯
NGC 3203	SA(r)0^{+}?	Boxy	In group	⋯
IC 4767	S pec	Peanut	In cluster	⋯
ESO 185- G 053	SB pec	Peanut	In cluster	⋯

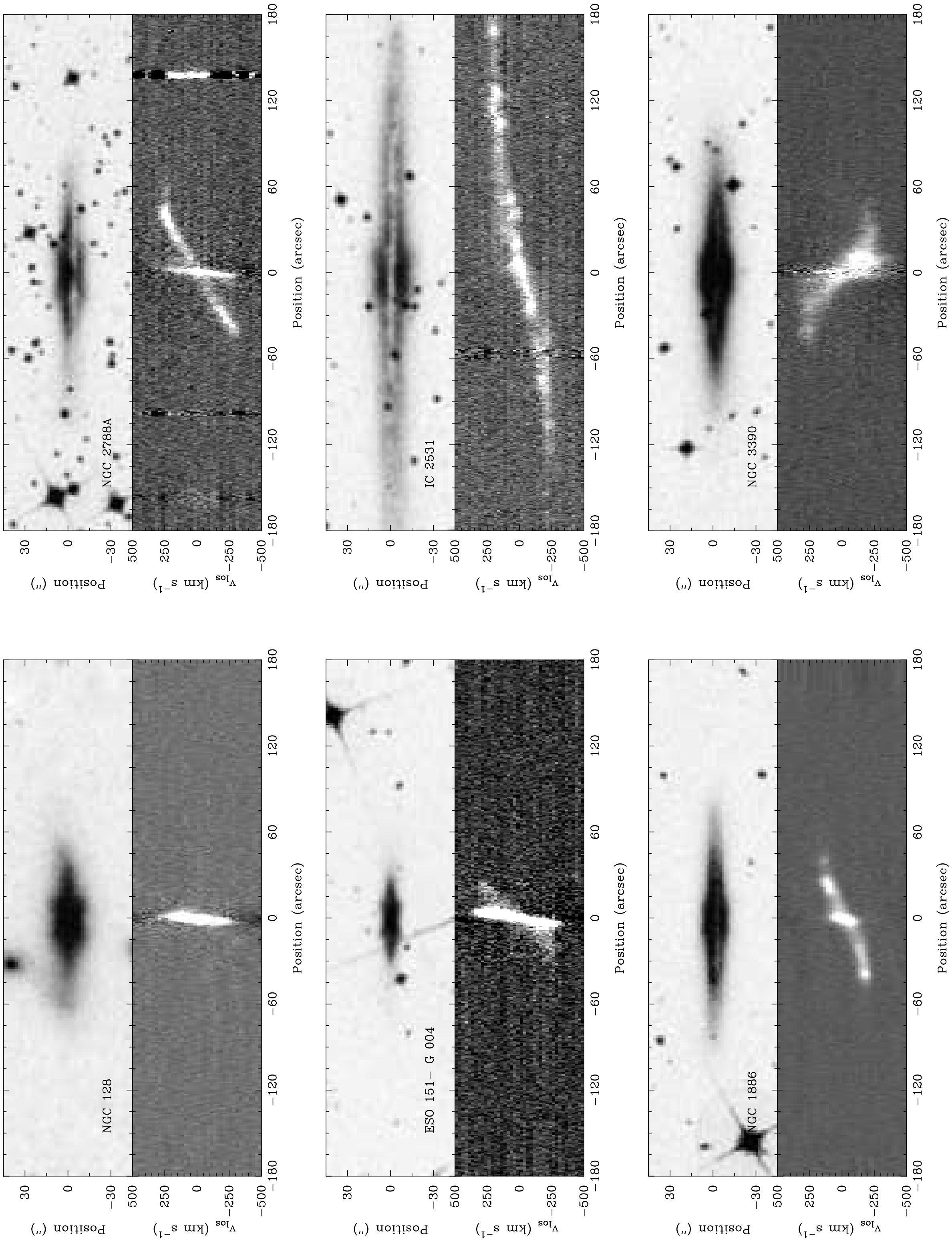
NGC 2788A
IC 2531
NGC 3390
NGC 128
ESO 151− G 004
NGC 1886
Position (arcsec)
Position (″)
v_{los} (km s^{-1})

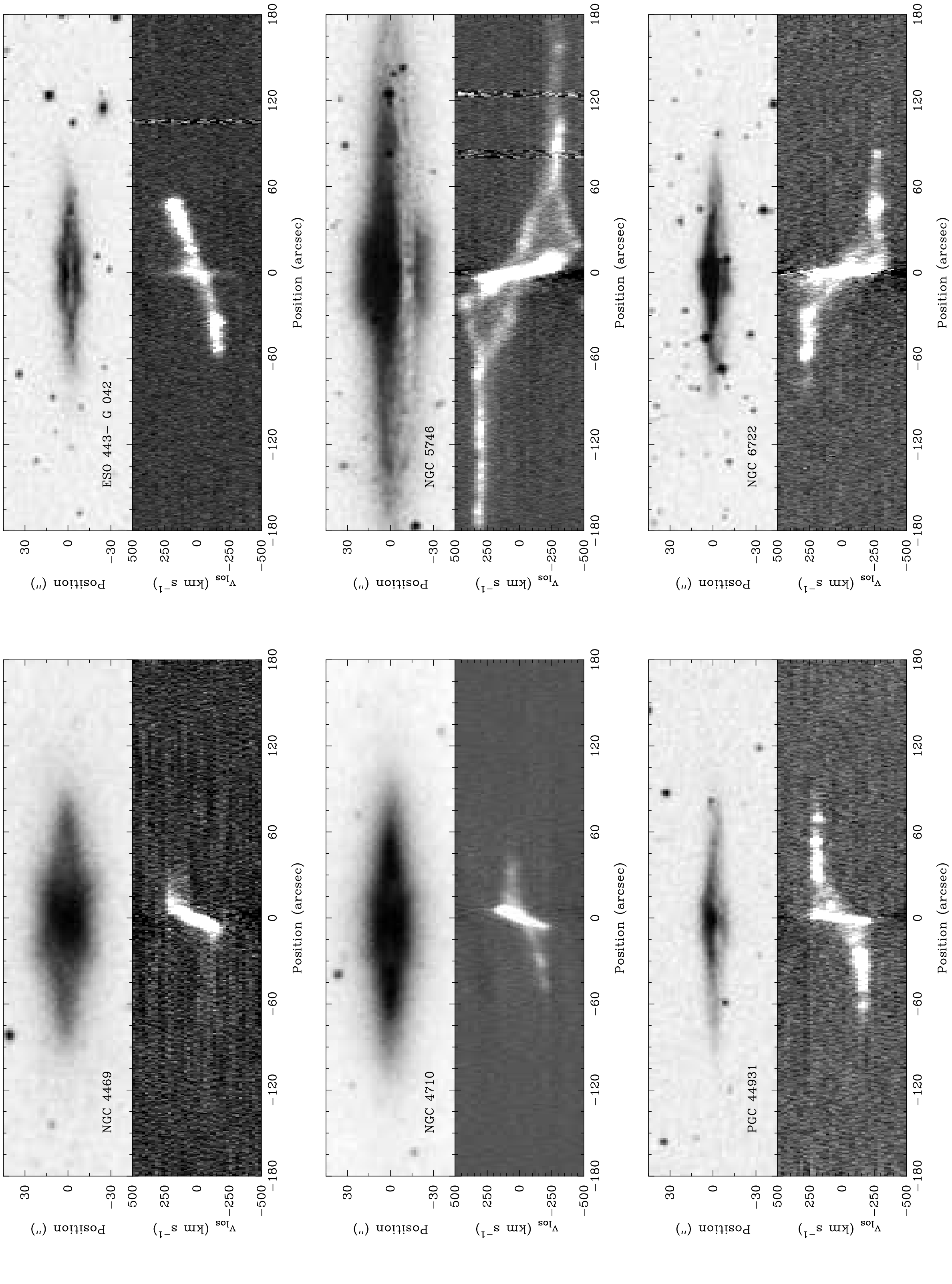

NGC 4469
NGC 4710
PGC 44931
ESO 443– G 042
NGC 5746
NGC 6722
Position (arcsec)
Position (″)
v_los (km s^-1)

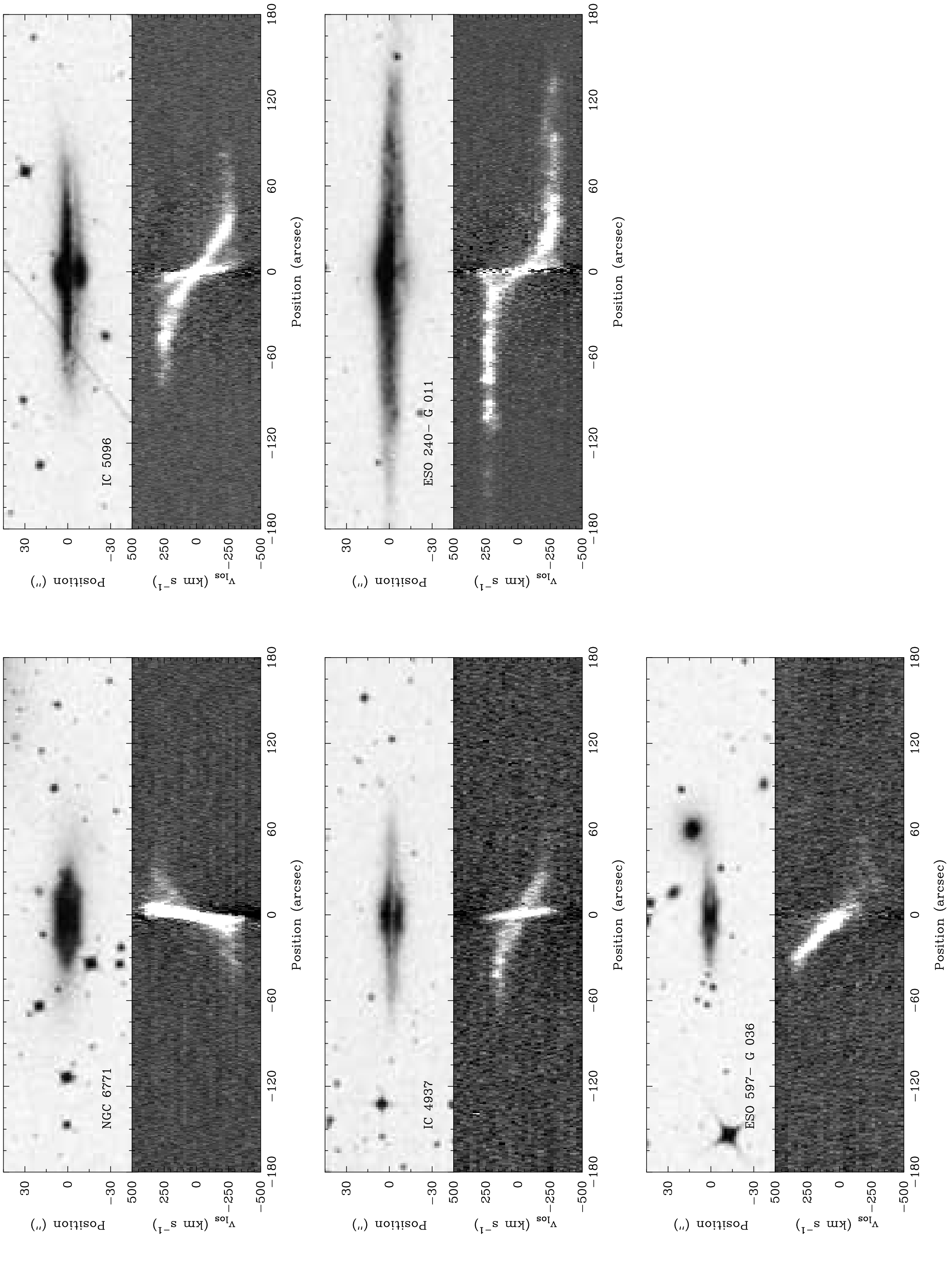
NGC 6771
IC 4937
ESO 597− G 036
IC 5096
ESO 240− G 011
Position (″)
v_los (km s^-1)
Position (arcsec)

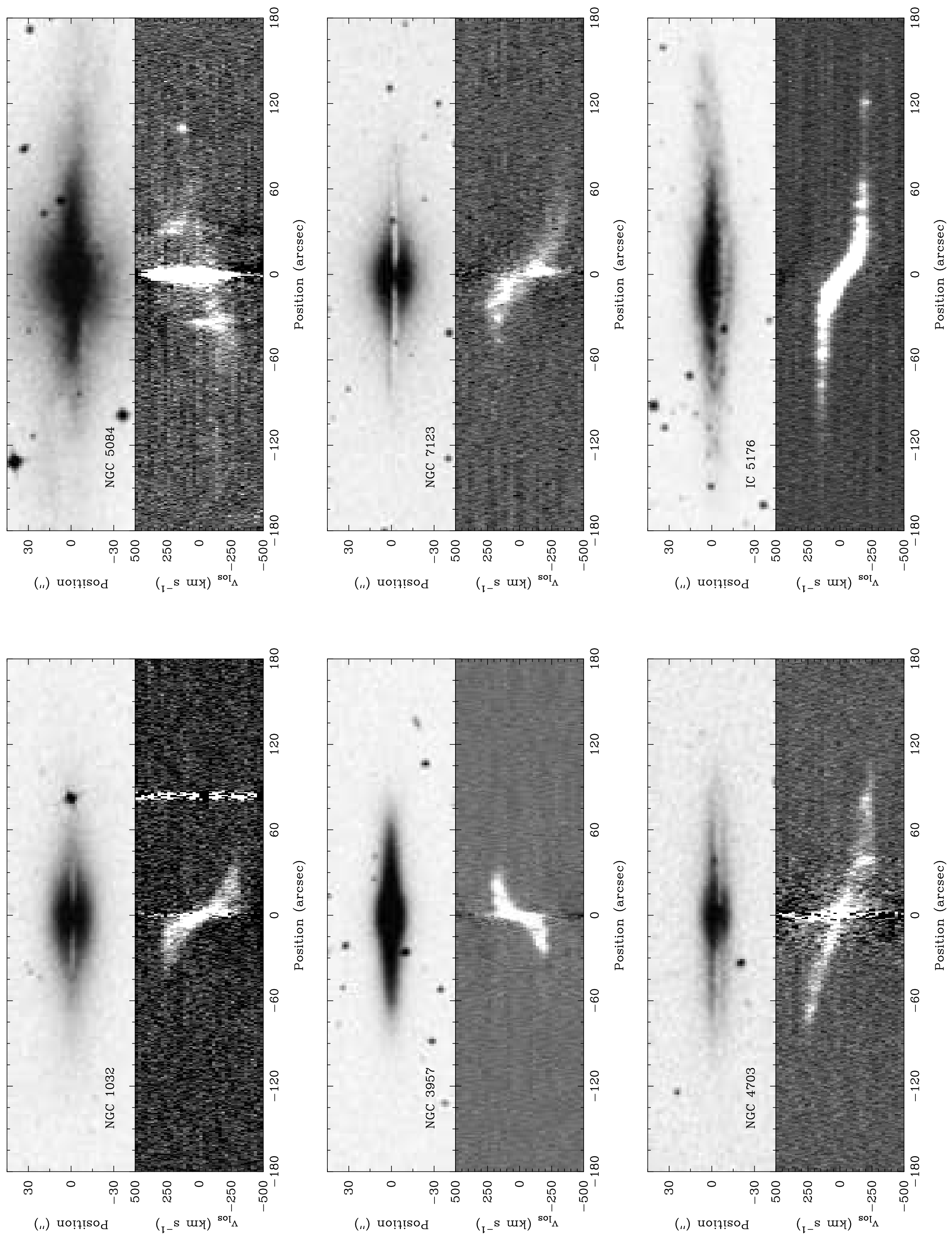
NGC 5084
NGC 1032
NGC 7123
NGC 3957
IC 5176
NGC 4703
Position (arcsec)
Position (″)
v$_{los}$ (km s^{-1})

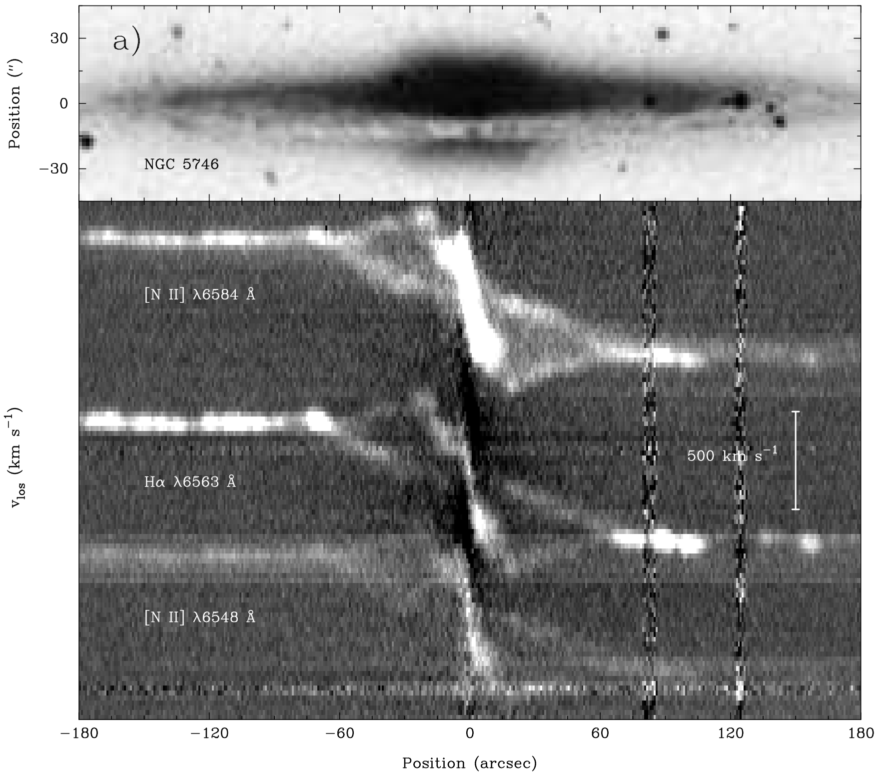
a)
NGC 5746
[N II] λ6584 Å
Hα λ6563 Å
[N II] λ6548 Å
500 km s^{-1}
Position (″)
v_{los} (km s^{-1})
Position (arcsec)

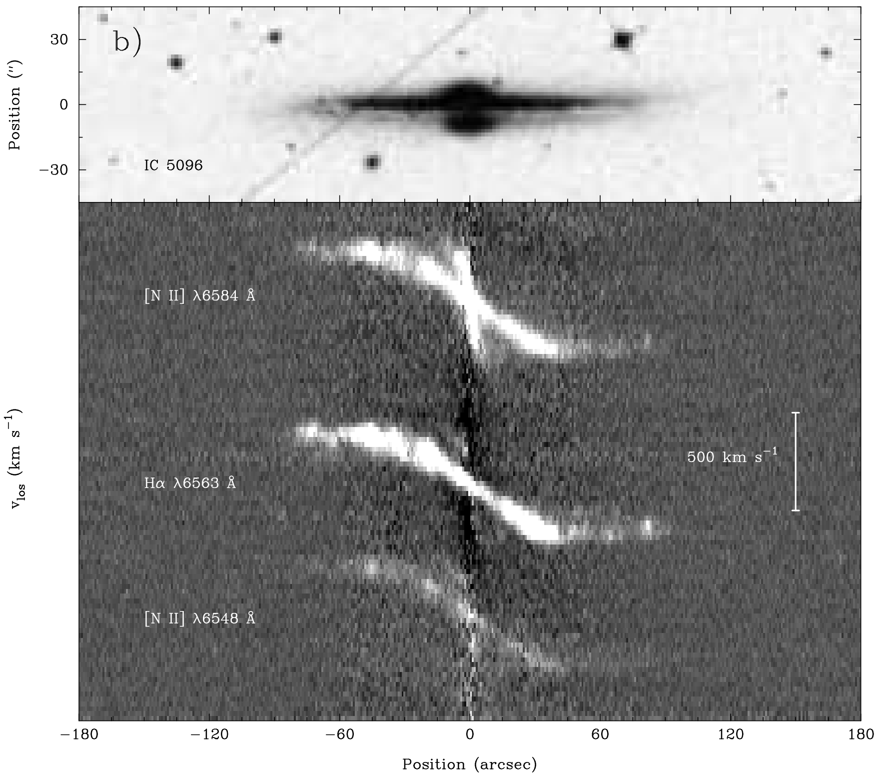
b)
IC 5096
[N II] λ6584 Å
Hα λ6563 Å
[N II] λ6548 Å
500 km s^{-1}
Position (″)
v_{los} (km s^{-1})
Position (arcsec)